Two particle states in an asymmetric box and the elastic scattering phases

Xu Feng, Xin Li, and Chuan Liu
Department of Physics, Peking University, Beijing, 100871, China
(Received 1 April 2004; published 29 July 2004)

The exact two-particle energy eigenstates in a generic asymmetric rectangular box with periodic boundary conditions in all three directions are studied. Their relations with the elastic scattering phases of the two particles in the continuum are obtained for both D_4 and D_2 symmetries. These results can be viewed as a generalization of the corresponding formulas in a cubic box obtained by Lüscher before. In particular, the *s*-wave scattering length is related to the energy shift in the finite box. Possible applications of these formulas are also discussed.

DOI: 10.1103/PhysRevD.70.014505 PACS number(s): 12.38.Gc, 11.15.Ha

I. INTRODUCTION

Scattering experiments serve as a major experimental tool in the study of interactions among particles. In these experiments, scattering cross sections are measured. By a partial-wave analysis, one obtains the experimental results on particle-particle scattering in terms of scattering phase shifts in a channel of definite quantum numbers. In the case of strong interactions, experimental results on hadron-hadron scattering phase shifts are available in the literature [1–5]. On the theoretical side, quantum chromodynamics (QCD) is believed to be the underlying theory of strong interactions. However, as a result of its nonperturbative nature, low-energy hadron-hadron scattering should be studied with a nonperturbative method. Lattice QCD provides a genuine nonperturbative method which can tackle these problems in principle, using numerical simulations. In a typical lattice calculation, energy eigenvalues of two-particle states with definite symmetry can be obtained by measuring appropriate correlation functions. Therefore, it would be desirable to relate these energy eigenvalues which are available through lattice calculations to the scattering phases which are obtained in the scattering experiment. This was accomplished in a series of papers by Lüscher [6–9] for a cubic box topology. In these references, especially Ref. [8], Lüscher found a nonperturbative relation of the energy of a two-particle state in a cubic box (a torus) with the corresponding elastic scattering phases of the two particles in the continuum. This formula, now known as Lüscher's formula, has been utilized in a number of applications—e.g., the linear sigma model in the broken phase [10] and also in quenched QCD [11–18]. As a result of limited numerical computational power, the *s*-wave scattering length, which is related to the scattering phase shift at vanishing relative three-momentum, is mostly studied in hadron scattering using a quenched approximation. The CP-PACS Collaboration calculated the scattering phases at nonzero momenta in pion-pion *s*-wave scattering in the $I=2$ channel [17] using quenched Wilson fermions and recently also in two-flavor full QCD [19].

In typical lattice QCD calculations, if one would like to probe for physical information concerning two-particle states with nonzero relative three-momentum, large lattices have to be used, which usually requires an enormous amount of computing resources. One of the reasons for this difficulty is the following. In a cubic box, the three-momenta of a single particle are quantized according to $\mathbf{k}=(2\pi/L)\mathbf{n}\equiv(2\pi/L)\times(n_1,n_2,n_3)$, with $\mathbf{n}\in\mathbb{Z}^3$.[1] In order to control lattice artifacts due to these nonzero momentum modes, one needs to have large values of L. One disadvantage of the cubic box is that the energy of a free particle with lowest nonzero momentum is degenerate. This means that the second lowest-energy level of the particle with nonvanishing momentum corresponds to $\mathbf{n}=(1,1,0)$. If one would like to measure these states on the lattice, even larger values of L should be used. One way to remedy this is to use a three-dimensional box whose shape is not cubic. If we use a *generic* rectangular box of size $(\eta_1 L)\times(\eta_2 L)\times L$ with η_1 and η_2 other than unity, we would have three different low-lying one-particle energies with nonzero momenta corresponding to $\mathbf{n}=(1,0,0)$, $(0,1,0)$, and $(0,0,1)$, respectively. This scenario is useful in practice since it presents more available low-momentum modes for a given lattice size, which is important in the study of hadron-hadron scattering phase shifts. In a recent analysis of nucleon-nucleon scattering on lattices, the authors of Ref. [20] also suggest the use of asymmetric volume lattices. A similar situation also occurs in the study of K to $\pi\pi$ matrix elements (see Ref. [21] for a review and references therein). There, one also needs to study two-particle states with nonvanishing relative three-momentum. Again, a cubic box yields too few available low-lying nonvanishing momenta and a large value of L is needed to reach the physical interesting kinematic region. In all of these cases, one could try an asymmetric rectangular box with only one side being large while the other sides moderate. One only has to choose the parameter η_1 and η_2 appropriately such that more low-lying momentum modes can be measure on the lattice with controllable lattice artifacts.

In an asymmetric rectangular box, the original formulas due to Lüscher, which give the relation between the energy eigenvalues of the two-particle states in the finite box and the continuum scattering phases, have to be modified accordingly. The purpose of this paper is to derive the equivalents of Lüscher's formulas in the case of a generic rectangular

---

[1] We use the notation $\mathbb{Z}^3$ to stand for the set of three-dimensional integers. That is, $\mathbf{n}\in\mathbb{Z}^3$ means that $\mathbf{n}=(n_1,n_2,n_3)$ with n_1, n_2, and n_3 integers.

 ©2004 The American Physical Society

(not necessarily cubic) box. Some results in this paper are also summarized in Ref. [22].

We consider two-particle states in a box of size $(\eta_1 L)\times(\eta_2 L)\times L$ with periodic boundary conditions in all three directions. For definiteness, we take $\eta_1 \geqslant 1, \eta_2 \geqslant 1$, which amounts to denoting the length of the smallest side of the rectangular box as L. The following derivation depends heavily on the previous results obtained in Ref. [8]. We will take over similar assumptions as in Ref. [8]. In particular, the relation between the energy eigenvalues and the scattering phases derived in the nonrelativistic quantum mechanical model can be carried over to the case of relativistic, massive field theory under these assumptions, the same way as in the case of cubic box which was discussed in detail in Ref. [8]. For the quantum mechanical model, we assume that the range of the interaction, denoted by R, of the two-particle system is such that $R<L/2$.

The modifications which have to be implemented, as compared with Ref. [8], are mainly concerned with different symmetries of the box. In a cubic box, the representations of the rotational group are decomposed into irreducible representations of the cubic group. In a generic asymmetric box, the symmetry of the system is reduced. In the case of $\eta_1 = \eta_2 \neq 1$, the basic group becomes D_4; if $\eta_1 \neq \eta_2 \neq 1$, the symmetry is further reduced to D_2, modulo parity operation. Therefore, the final expression relating the energy eigenvalues of the system and the scattering phases will be different.

This paper is organized as follows. In Sec. II, we discuss the singular periodic solutions to the Helmholtz equation. The energy eigenstates of the two-particle system can be expanded in terms of these solutions. In Sec. III, we discuss in detail the symmetry of an asymmetric box. Two cases are studied: $\eta_1 = \eta_2$ in which case the basic symmetry group is D_4 and $\eta_1 \neq \eta_2$ in which case the symmetry group is D_2. The irreducible representations of the rotational group are decomposed into irreducible representations of these point groups. Energy eigenvalues in the A_1^+ sector are related to the scattering phases for the two cases, respectively. In Sec. IV, we discuss the low-momentum and large-volume limit of the general formulas obtained in Sec. III. A simplified formula is obtained for the scattering length and numerical values for the coefficients of this expansion are listed. Finally, in Sec. V, we conclude with some general remarks. Some details of the calculation are provided in the Appendixes for reference.

II. ENERGY EIGENSTATES AND SINGULAR PERIODIC SOLUTIONS OF THE HELMHOLTZ EQUATION

Our notation close follows that used in Ref. [8]. The energy eigenstates in a periodic box is intimately related to the singular periodic solutions of the Helmholtz equation:

$$(\nabla^2 + k^2)\psi(\mathbf{r}) = 0. \tag{1}$$

If the function $\psi(\mathbf{r})$ is a solution to the Helmholtz equation for $\mathbf{r}\neq 0$ and it is periodic $\psi(\mathbf{r}+\hat{\mathbf{n}}L)=\psi(\mathbf{r})$ satisfies $\sup_{0<r<L/2} r^{\Lambda+1}\psi(\mathbf{r})<\infty$ for some integer Λ, we call $\psi(\mathbf{r})$ a singular periodic solution to the Helmholtz equation of degree Λ.

The momentum modes in the rectangular box are quantized as $\mathbf{k}=(2\pi/L)\tilde{\mathbf{n}}$. For every $\mathbf{n}=(n_1,n_2,n_3)\in\mathbb{Z}^3$, we introduce the notation

$$\tilde{\mathbf{n}} \equiv (n_1/\eta_1, n_2/\eta_2, n_3), \quad \hat{\mathbf{n}} \equiv (n_1\eta_1, \eta_2 n_2, n_3). \tag{2}$$

When discussing the singular periodic solutions to the Helmholtz equation, one should differentiate two cases: regular values of k, which means that $|k|\neq(2\pi/L)|\tilde{\mathbf{n}}|$ for any $\mathbf{n}\in\mathbb{Z}^3$, and singular values of k, which means that $|k| = (2\pi/L)|\tilde{\mathbf{n}}|$ for some $\mathbf{n}\in\mathbb{Z}^3$. For our purposes, it suffices to study the regular values of k. In this case, the singular periodic solutions of Helmholtz equation can be obtained from the Green's function

$$G(\mathbf{r};k^2) = \frac{1}{\eta_1\eta_2 L^3}\sum_{\mathbf{p}} \frac{e^{i\mathbf{p}\cdot\mathbf{r}}}{\mathbf{p}^2-k^2}, \tag{3}$$

where the summation over $\mathbf{p}$ runs over all possible momenta in the rectangular box: $\mathbf{p}=(2\pi/L)\tilde{\mathbf{n}}$. One can easily check that the function $G(\mathbf{r};k^2)$ is a singular periodic solution of the Helmholtz equation with degree 1. More singular periodic solutions can be obtained as follows. We define

$$\mathcal{Y}_{lm}(\mathbf{r}) \equiv r^l Y_{lm}(\Omega_{\mathbf{r}}), \tag{4}$$

where $\Omega_{\mathbf{r}}$ represents the solid angle parameters (θ,ϕ) of $\mathbf{r}$ in spherical coordinates; Y_{lm} are the usual spherical harmonic functions. It is well known that $\mathcal{Y}_{lm}(\mathbf{r})$ consist of all linear independent, homogeneous functions in (x,y,z) of degree l that transform irreducibly under the rotational group. We then define

$$G_{lm}(\mathbf{r};k^2) = \mathcal{Y}_{lm}(\nabla) G(\mathbf{r};k^2). \tag{5}$$

One can show that the functions $G_{lm}(\mathbf{r};k^2)$ form a complete, linear independent set of functions of singular periodic solutions of the Helmholtz equation with degree l. That is to say, any singular periodic solution of the Helmholtz equation with degree Λ is given by

$$\psi(\mathbf{r}) = \sum_{l=0}^{\Lambda}\sum_{m=-l}^{l} v_{lm} G_{lm}(\mathbf{r},k^2), \tag{6}$$

with complex coefficients v_{lm}. The functions $G_{lm}(\mathbf{r};k^2)$ may be expanded into usual spherical harmonics with the result

$$G_{lm}(\mathbf{r};k^2) = \frac{(-)^l k^{l+1}}{4\pi}\bigg[Y_{lm}(\Omega_{\mathbf{r}}) n_l(kr) + \sum_{l'm'} \mathcal{M}_{lm;l'm'} Y_{l'm'}(\Omega_{\mathbf{r}}) j_{l'}(kr)\bigg]. \tag{7}$$

Here, j_l and n_l are the usual spherical Bessel functions and the matrix $\mathcal{M}_{lm;l'm'}$ is related to the *modified* zeta function via

$$\mathcal{M}_{lm;js}=\sum_{l'm'}\frac{(-)^s i^{j-l}\mathcal{Z}_{l'm'}(1,q^2;\eta_1,\eta_2)}{\eta_1\eta_2\pi^{3/2}q^{l'+1}}\times\sqrt{(2l+1)(2l'+1)(2j+1)}\begin{pmatrix} l & l' & j\\ 0 & 0 & 0\end{pmatrix}\times\begin{pmatrix} l & l' & j\\ m & m' & -s\end{pmatrix}, \quad (8)$$

where $q=kL/(2\pi)$. In this formula, the Wigner $3j$ symbols can be related to the Clebsch-Gordan coefficients in the usual way [23]. For a given angular momentum cutoff Λ, the quantity $\mathcal{M}_{lm;l'm'}$ can be viewed as the matrix element of a linear operator $\hat{M}$ in a vector space $\mathcal{H}_\Lambda$, which is spanned by all harmonic polynomials of degree $l\leqslant\Lambda$. The modified zeta function is formally defined by

$$\mathcal{Z}_{lm}(s,q^2;\eta_1,\eta_2)=\sum_{\mathbf{n}}\frac{\mathcal{Y}_{lm}(\tilde{\mathbf{n}})}{(\tilde{\mathbf{n}}^2-q^2)^s}. \quad (9)$$

According to this definition, the summation at the right-hand side of Eq. (9) is formally divergent for $s=1$ and needs to be analytically continued. Following similar discussions as in Ref. [8], one could obtain a finite expression for the modified zeta function which is suitable for numerical evaluation. Explicit formulas for $\mathcal{Z}_{lm}(s,q^2;\eta_1,\eta_2)$ at $s=1$ and $s=2$ are derived in Appendix A. From the analytically continued formula, it is obvious from the symmetry of D_4 or D_2 that, for $l\leqslant 4$, the only nonvanishing zeta functions at $s=1$ are $\mathcal{Z}_{00}$, $\mathcal{Z}_{20}$, $\mathcal{Z}_{2\pm2}$, $\mathcal{Z}_{40}$, $\mathcal{Z}_{4\pm2}$, and $\mathcal{Z}_{4\pm4}$. It is also easy to verify that, if $\eta_1=\eta_2=1$, all of the above definitions and formulas reduce to the those obtained in Ref. [8].

In the region where the interaction is vanishing, the energy eigenstates of the two-particle system can be expressed in terms of ordinary spherical Bessel functions

$$\psi_{lm}(r)=b_{lm}[\alpha_l(k)j_l(kr)+\beta_l(k)n_l(kr)], \quad (10)$$

for some constants b_{lm}. Also, this energy eigenfunction coincides with a singular periodic solution of the Helmholtz equation in this region. Comparison of Eq. (10) with Eq. (7) then yields

$$b_{lm}\alpha_l(k)=\sum_{l'=0}^{\Lambda}\sum_{m'=-l'}^{l'}v_{l'm'}\frac{(-)^{l'}k^{l'+1}}{4\pi}\mathcal{M}_{l'm';lm},$$

$$b_{lm}\beta_l(k)=v_{lm}\frac{(-)^l k^{l+1}}{4\pi}, \quad (11)$$

with $l=0,1,\ldots,\Lambda$. Note that this equation can be viewed as a linear equation in a vector space $\mathcal{H}_\Lambda$, which is the space of all complex vectors whose components are v_{lm} with $l=0,1,\ldots,\Lambda$ and $m=-l,\ldots,l$. The matrix elements $\mathcal{M}_{l'm';lm}$ can be viewed as the matrix element of an operator M in vector space $\mathcal{H}_\Lambda$. The scattering phases of the two particles are related to the coefficients $\alpha_l(k)$ and $\beta_l(k)$ via

$$e^{2i\delta_l(k)}=\frac{\alpha_l(k)+i\beta_l(k)}{\alpha_l(k)-i\beta_l(k)}. \quad (12)$$

Therefore, nontrivial solution to Eq. (11) requires that

$$\det[e^{2i\delta}-U]=0, \quad U=(M+i)/(M-i). \quad (13)$$

This gives the general relation between the energy eigenvalue of a two-particle eigenstate in a finite box with the corresponding scattering phases.

III. SYMMETRY OF AN ASYMMETRIC BOX

The general result (13) obtained in the previous section can be further simplified when we consider irreducible representations of the symmetry group of the box. We know that energy eigenstates in a box can be characterized by their transformation properties under the symmetry group of the box. For this purpose, one has to decompose the representations of the rotational group with angular momentum l into irreducible representations of the corresponding symmetry group of the box. For an asymmetric box, the relevant symmetry group is either D_4 if $\eta_1=\eta_2\neq 1$ or D_2 if $\eta_1\neq\eta_2\neq 1$. In a given symmetry sector, denoted by its irreducible representation Γ, the representation of the rotational group with angular momentum l is decomposed into irreducible representations of D_4 or D_2. This decomposition may contain the irreducible representation Γ. We may pick our basis as $|\Gamma,\alpha;l,n\rangle$. Here α runs from 1 to $\dim(\Gamma)$, the dimension of the irreducible representation Γ. Label n runs from 1 to the total number of occurrence of Γ in the decomposition of rotational group representation with angular momentum l. The matrix $\hat{M}$ is diagonal with respect to Γ and α by Schur's lemma. For convenience, we have listed these basis polynomials in terms of spherical harmonics $\mathcal{Y}_{lm}(\mathbf{r})$ in Table I. In this table, in order to make the notation more compact, we have used one single label—i.e., the label of the angular momentum—to designate a basis vector. Different basis vectors with the same angular momentum are differentiated by adding a dot, a circle, etc., either on top of or below the corresponding label.

For the two-particle eigenstate in the symmetry sector Γ in a box of particular symmetry (either D_4 or D_2), the energy eigenvalue, $E=k^2/(2\mu)$ with μ being the reduced mass of the two particles, is determined by

$$\det[e^{2i\delta}-\hat{U}(\Gamma)]=0, \quad \hat{U}(\Gamma)=[\hat{M}(\Gamma)+i]/[\hat{M}(\Gamma)-i]. \quad (14)$$

Here $\hat{M}(\Gamma)$ represents a linear operator in the vector space $\mathcal{H}_\Lambda(\Gamma)$. This vector space is spanned by all complex vectors whose components are v_{ln}, with $l\leqslant\Lambda$, and n runs from 1 to the number of occurrence of Γ in the decomposition of representation with angular momentum l [8]. To write out more explicit formulas, one therefore has to consider decompositions of the rotational group representations under appropriate symmetries.

TABLE I. Basis polynomials in terms of spherical harmonics for various irreducible representations Γ of the symmetry groups D_4 and D_2 up to angular momentum $l=4$.

	Group D_4		Group D_2	
l	Γ	Basis polynomials	Γ	Basis polynomials
0	A_1^+	$\|0\rangle$	A^+	$\|0\rangle=\mathcal{Y}_{00}$
1	A_2^-	$\|1\rangle$	B_1^-	$\|1\rangle=\mathcal{Y}_{10}$
	E^-	$(\|\tilde{1}\rangle,\|\underset{\sim}{1}\rangle)$	B_2^- ; B_3^-	$\|\tilde{1}\rangle=(\mathcal{Y}_{11}+\mathcal{Y}_{1-1})$; $\|\underset{\sim}{1}\rangle=(\mathcal{Y}_{11}-\mathcal{Y}_{1-1})$
2	A_1^+	$\|2\rangle$	A^+	$\|2\rangle=\mathcal{Y}_{20}$
	E^+	$(\|\tilde{2}\rangle,\|\underset{\sim}{2}\rangle)$	B_3^+ ; B_2^+	$\|\tilde{2}\rangle=(\mathcal{Y}_{21}+\mathcal{Y}_{2-1})$; $\|\underset{\sim}{2}\rangle=(\mathcal{Y}_{21}-\mathcal{Y}_{2-1})$
	B_1^+ ; B_2^+	$\|\bar{2}\rangle$; $\|\underline{2}\rangle$	A^+; B_1^+	$\|\bar{2}\rangle=(\mathcal{Y}_{22}+\mathcal{Y}_{2-2})$; $\|\underline{2}\rangle=(\mathcal{Y}_{22}-\mathcal{Y}_{2-2})$
3	A_2^-	$\|3\rangle$	B_1^-	$\|3\rangle=\mathcal{Y}_{30}$
	E^-	$(\|\tilde{3}\rangle,\|\underset{\sim}{3}\rangle)$	B_2^- ; B_3^-	$\|\tilde{3}\rangle=(\mathcal{Y}_{31}+\mathcal{Y}_{3-1})$; $\|\underset{\sim}{3}\rangle=(\mathcal{Y}_{31}-\mathcal{Y}_{3-1})$
	B_2^- ; B_1^-	$\|\bar{3}\rangle$; $\|\underline{3}\rangle$	B_1^- ; A^-	$\|\bar{3}\rangle=(\mathcal{Y}_{32}+\mathcal{Y}_{3-2})$; $\|\underline{3}\rangle=(\mathcal{Y}_{32}-\mathcal{Y}_{3-2})$
	E^-	$(\|\dot{3}\rangle,\|\underset{\cdot}{3}\rangle)$	B_2^- ; B_3^-	$\|\dot{3}\rangle=(\mathcal{Y}_{33}+\mathcal{Y}_{3-3})$; $\|\underset{\cdot}{3}\rangle=(\mathcal{Y}_{33}-\mathcal{Y}_{3-3})$
4	A_1^+	$\|4\rangle$	A^+	$\|4\rangle=\mathcal{Y}_{40}$
	E^+	$(\|\tilde{4}\rangle,\|\underset{\sim}{4}\rangle)$	B_3^+ ; B_2^+	$\|\tilde{4}\rangle=(\mathcal{Y}_{41}+\mathcal{Y}_{4-1})$; $\|\underset{\sim}{4}\rangle=(\mathcal{Y}_{41}-\mathcal{Y}_{4-1})$
	B_1^+ ; B_2^+	$\|\bar{4}\rangle$; $\|\underline{4}\rangle$	A^+; B_1^+	$\|\bar{4}\rangle=(\mathcal{Y}_{42}+\mathcal{Y}_{4-2})$; $\|\underline{4}\rangle=(\mathcal{Y}_{42}-\mathcal{Y}_{4-2})$
	E^+	$(\|\dot{4}\rangle,\|\underset{\cdot}{4}\rangle)$	B_3^+ ; B_2^+	$\|\dot{4}\rangle=(\mathcal{Y}_{43}+\mathcal{Y}_{4-3})$; $\|\underset{\cdot}{4}\rangle=(\mathcal{Y}_{43}-\mathcal{Y}_{4-3})$
	A_1^+ ; A_2^+	$\|\mathring{4}\rangle$; $\|\underset{\circ}{4}\rangle$	A^+; B_1^+	$\|\mathring{4}\rangle=(\mathcal{Y}_{44}+\mathcal{Y}_{4-4})$; $\|\underset{\circ}{4}\rangle=(\mathcal{Y}_{44}-\mathcal{Y}_{4-4})$

We first consider the case $\eta_1=\eta_2$. The basic symmetry group is D_4, which has 4 one-dimensional (irreducible) representations A_1, A_2, B_1, B_2 and a two-dimensional irreducible representation E.[2] The representations of the rotational group are decomposed according to

$$\begin{aligned}
\mathbf{0}&=A_1^+,\\
\mathbf{1}&=A_2^-+E^-,\\
\mathbf{2}&=A_1^++B_1^++B_2^++E^+,\\
\mathbf{3}&=A_2^-+B_1^-+B_2^-+E^-+E^-,\\
\mathbf{4}&=A_1^++A_1^++A_2^++B_1^++B_2^++E^++E^+.
\end{aligned} \tag{15}$$

In most lattice calculations, the symmetry sector that is easiest to investigate is the invariant sector A_1^+. We therefore will focus on this particular symmetry sector. We see from Eq. (15) that, up to $l\leqslant 4$, s waves, d waves, and g waves contribute to this sector. This corresponds to *four* linearly independent, homogeneous polynomials with degrees not more than 4, which are invariant under D_4. From Table I we see that the four polynomials can be identified as the basis $|0\rangle$, $|2\rangle$, $|4\rangle$, and $|\mathring{4}\rangle$, respectively.[3] Therefore, we can write out the four-dimensional reduced matrix $\mathcal{M}(A_1^+)$ whose matrix elements are denoted as $\mathcal{M}(A_1^+)_{ll'}=m_{ll'}=m_{l'l}$, where l and l' takes values in 0, 2, 4, and $\mathring{4}$, respectively. Using the general formula (8), it is straightforward to work out these reduced matrix elements in terms of matrix elements $\mathcal{M}_{lm;l'm'}$. These are given explicitly in Appendix B. We find that, in the case of D_4 symmetry, Eq. (14) becomes

$$\begin{vmatrix}
\cot\delta_0-m_{00} & m_{02} & m_{04} & m_{0\mathring{4}}\\
m_{20} & \cot\delta_2-m_{22} & m_{24} & m_{2\mathring{4}}\\
m_{40} & m_{42} & \cot\delta_4-m_{44} & m_{4\mathring{4}}\\
m_{\mathring{4}0} & m_{\mathring{4}2} & m_{\mathring{4}4} & \cot\delta_4-m_{\mathring{4}\mathring{4}}
\end{vmatrix}=0. \tag{16}$$

For the case $\eta_1\neq\eta_2$, the symmetry group becomes D_2 which has only 4 one-dimensional irreducible representations A, B_1, B_2, and B_3. The decomposition (15) is replaced by

[2]The notations of the irreducible representations of groups D_4 and D_2 that we adopt here are taken from Ref. [24], Chap. XII.
[3]Our conventions for the spherical harmonics are taken from Ref. [25].

$$
\begin{aligned}
\mathbf{0} &= A^{+}, \\
\mathbf{1} &= B_1^{-}+B_2^{-}+B_3^{-}, \\
\mathbf{2} &= A^{+}+A^{+}+B_1^{+}+B_2^{+}+B_3^{+}, \\
\mathbf{3} &= A^{-}+B_1^{-}+B_1^{-}+B_2^{-}+B_2^{-}+B_3^{-}+B_3^{-}, \\
\mathbf{4} &= A^{+}+A^{+}+A^{+}+B_1^{+}+B_1^{+}+B_2^{+}+B_2^{+}+B_3^{+}+B_3^{+}.
\end{aligned}
\tag{17}
$$

So, up to $l \leqslant 4$, A^+ occurs *six* times: once in $l=0$, twice in $l=2$ and three times in $l=4$. The corresponding basis polynomials can be taken as $|0\rangle$, $|2\rangle$, $|\overline{2}\rangle$, $|4\rangle$, $|\overline{4}\rangle$, and $|\mathring{4}\rangle$, respectively. The reduced matrix $\hat{M}(A^+)$ is six dimensional with matrix elements $\mathcal{M}_{ll'}=m_{ll'}$. The explicit expressions for these matrix elements can by found in Appendix B. The relation between the energy eigenvalue and the scattering phase is similar to Eq. (16) except that the matrix becomes a 6×6 matrix

$$
\begin{vmatrix}
\xi_0-m_{00} & m_{02} & m_{0\bar{2}} & m_{04} & m_{0\bar{4}} & m_{0\mathring{4}} \\
m_{20} & \xi_2-m_{22} & m_{2\bar{2}} & m_{24} & m_{2\bar{4}} & m_{2\mathring{4}} \\
m_{\bar{2}0} & m_{\bar{2}2} & \xi_2-m_{\bar{2}\bar{2}} & m_{\bar{2}4} & m_{\bar{2}\bar{4}} & m_{\bar{2}\mathring{4}} \\
m_{40} & m_{42} & m_{4\bar{2}} & \xi_4-m_{44} & m_{4\bar{4}} & m_{4\mathring{4}} \\
m_{\bar{4}0} & m_{\bar{4}2} & m_{\bar{4}\bar{2}} & m_{\bar{4}4} & \xi_4-m_{\bar{4}\bar{4}} & m_{\bar{4}\mathring{4}} \\
m_{\mathring{4}0} & m_{\mathring{4}2} & m_{\mathring{4}\bar{2}} & m_{\mathring{4}4} & m_{\mathring{4}\bar{4}} & \xi_4-m_{\mathring{4}\mathring{4}}
\end{vmatrix} = 0,
\tag{18}
$$

where we have used the simplified notation $\xi_l(q)=\cot\,\delta_l(q)$. In principle, if even higher angular momentum is desired, similar formulas can be derived.

IV. LOW-MOMENTUM EXPANSION AND THE SCATTERING LENGTH

Usually, scattering phases with higher angular momentum are much smaller than phases with lower angular momentum. This is particularly true in low-momentum scattering. It is well known that for small relative momentum k, the scattering phases behave like

$$
\tan\,\delta_l(k) \sim a_l k^{2l+1},
\tag{19}
$$

for small k. Therefore, we anticipate that in the low-momentum limit, scattering phases with small l will dominate the scattering process. If we treat the d-wave and g-wave scattering phases as small perturbations, we find that for the D_4 symmetry, Eq. (16) can be simplified to

$$
\cot\,\delta_0 - m_{00} = \frac{m_{02}^2}{\cot\,\delta_2 - m_{22}} + \frac{m_{04}^2}{\cot\,\delta_4 - m_{44}} + \frac{m_{0\bar{4}}^2}{\cot\,\delta_4 - m_{\bar{4}\bar{4}}}.
\tag{20}
$$

For the symmetry D_2, similar to Eq. (20), Eq. (18) reads

$$
\cot\,\delta_0 - m_{00} = \frac{m_{02}^2}{\cot\,\delta_2 - m_{22}} + \frac{m_{0\bar{2}}^2}{\cot\,\delta_2 - m_{\bar{2}\bar{2}}} + \frac{m_{04}^2}{\cot\,\delta_4 - m_{44}} + \frac{m_{0\tilde{4}}^2}{\cot\,\delta_4 - m_{\tilde{4}\tilde{4}}} + \frac{m_{0\bar{4}}^2}{\cot\,\delta_4 - m_{\bar{4}\bar{4}}}.
\tag{21}
$$

If the d-wave and g-wave phase shifts were small enough, it is easy to check that both Eqs. (20) and (21) simplify to

$$
\cot\,\delta_0(k) = m_{00} = \frac{\mathcal{Z}_{00}(1,q^2;\eta_1,\eta_2)}{\pi^{3/2}\eta_1\eta_2 q}.
\tag{22}
$$

For the general case, Eqs. (20) and (21) offer the desired relation between the energy eigenvalues in the A_1^+ sector and the scattering phases for the cases $\eta_1=\eta_2$ and $\eta_1\neq\eta_2$, respectively. It is easy to verify that, in both Eqs. (20) and (21), contributions that appear in the right-hand side of the equations are smaller by a factor of q^2 compared with m_{00} on the left-hand side. They are negligible as long as the relative momentum q is small enough. Therefore, in both cases, the s-wave scattering length a_0 will be determined by the zero momentum limit of Eq. (22).

It is also possible to work out the corrections due to higher scattering phases to the s-wave scattering phase. For example, we have

$$
n\pi - \delta_0(q) = \phi(q) + \sigma_2(q)\tan\,\delta_2(q) + \sigma_4(q)\tan\,\delta_4(q),
\tag{23}
$$

where the angle $\phi(q)$ is defined via $-\tan\,\phi(q)=1/m_{00}(q)$. The functions $\sigma_2(q)$ and $\sigma_4(q)$ represent the sensitivity of higher scattering phases. For D_4 and D_2 symmetries, they are given by

$$
\sigma_2(q) = \begin{cases} m_{02}^2/(1+m_{00}^2), & \text{for group } D_4, \\ (m_{02}^2+m_{0\bar{2}}^2)/(1+m_{00}^2), & \text{for group } D_2, \end{cases}
\tag{24}
$$

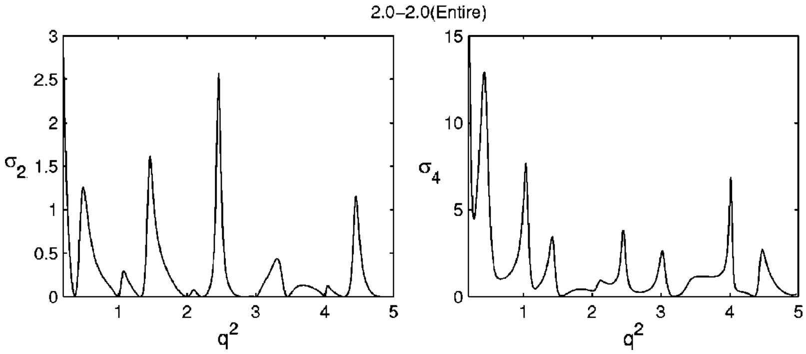

FIG. 1. The functions $\sigma_2(q^2)$ and $\sigma_4(q^2)$ as a function of q^2 are plotted for both D_4 symmetries with parameters $\eta_1 = \eta_2 = 2$.

$$\sigma_4(q) = \begin{cases} (m_{04}^2 + m_{0\bar{4}}^2)/(1+m_{00}^2), & \text{for group } D_4, \\ (m_{04}^2 + m_{0\bar{4}}^2 + m_{0\tilde{4}}^2)/(1+m_{00}^2), & \text{for group } D_2. \end{cases} \tag{25}$$

The functions $\sigma_2(q^2)$ and $\sigma_4(q^2)$ can be calculated using the matrix elements given in Appendix B. In Figs. 1 and 2, these functions are plotted versus q^2 for the case of D_4 symmetry ($\eta_1 = \eta_2 = 2$) and for the case of D_2 with $\eta_1 = 2.0$, $\eta_2 = 1.5$, respectively. It is seen that the functions $\sigma_2(q^2)$ and $\sigma_4(q^2)$ remain finite for all $q^2 > 0$. For some particular values of q^2, however, these functions can become quite large in magnitude. This is due to almost coincidence of singularities of the numerator and denominator in matrix elements m_{0i} which happens for some choices of η_1 and η_2. For values of q^2 away from these values, the functional values of σ_2 and σ_4 remain moderate. In Fig. 2, the lower two panels in the plot are simply the same function as in the upper panels with the scale of the vertical axis being magnified, in order to show the detailed variation of the functions.

We remark here that, in principle, the corrections due to scattering phases with higher l can be estimated from lattice calculations as well. From Table I it is seen that, for lattices with D_4 symmetry, by inspecting energy eigenstates with E^+, B_1^+, or B_2^+ symmetry on the lattice, one can get an estimate for the d-wave scattering phase δ_2 which dominates these symmetry sectors. Similarly, for lattices with D_2 symmetry, the eigenstates with B_1^+, B_2^+, or B_3^+ symmetry should be studied. It is also interesting to note that for lattices with D_4 symmetry, if we study the eigenstates with A_2^+ symmetry, then the leading contribution comes from g-wave scattering phase δ_4.

We now come to the discussion of scattering length. For a large box, a large L expansion of the formulas can be de-

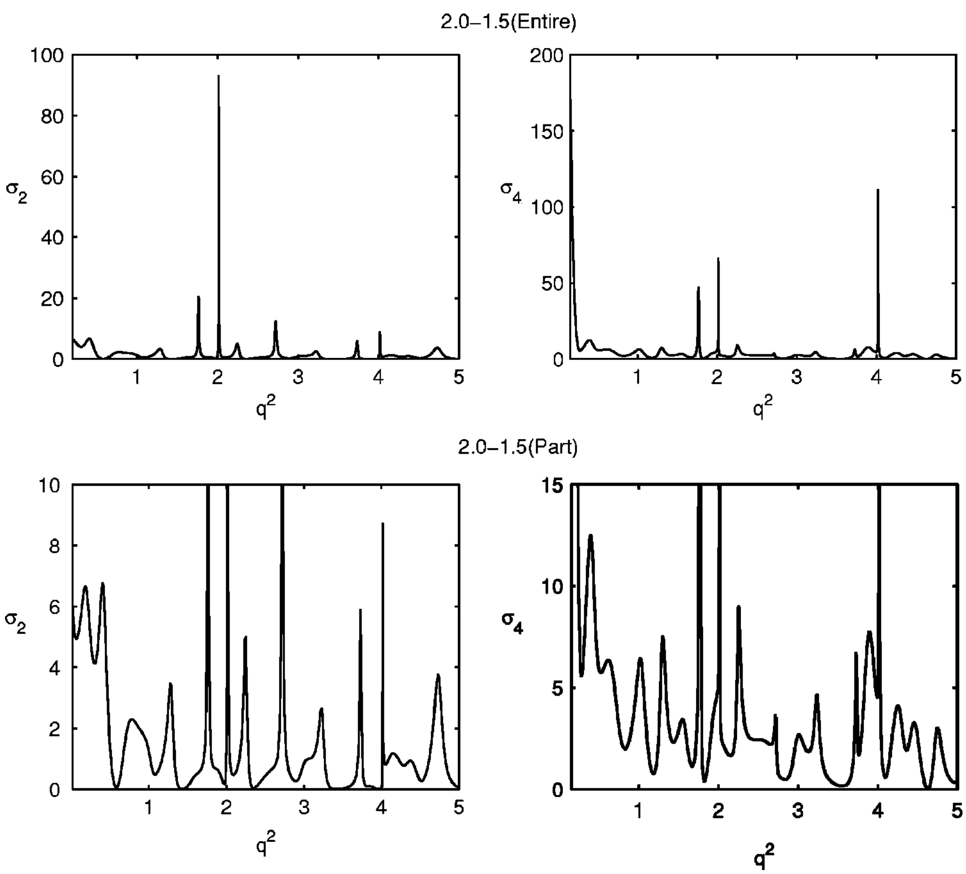

FIG. 2. The functions $\sigma_2(q^2)$ and $\sigma_4(q^2)$ as a function of q^2 are plotted for both D_2 symmetries with parameters $\eta_1 = 2$, $\eta_2 = 1.5$.

TABLE II. Numerical values for the subtracted zeta functions and the coefficients $c_1(\eta_1,\eta_2)$ and $c_2(\eta_1,\eta_2)$ under some typical topology. The three-dimensional rectangular box has a size $L_1=\eta_1 L$, $L_2=\eta_2 L$, and $L_3=L$.

L_1:L_2:L_3	η_1	η_2	$\hat{Z}_{00}(1,0;\eta_1,\eta_2)$	$\hat{Z}_{00}(2,0;\eta_1,\eta_2)$	$c_1(\eta_1,\eta_2)$	$c_2(\eta_1,\eta_2)$
1:1:1	1	1	−8.913633	16.532316	−2.837297	6.375183
6:5:4	1.5	1.25	−12.964476	41.526870	−2.200918	3.647224
4:3:2	2	1.5	−16.015122	91.235227	−1.699257	1.860357
3:2:2	1.5	1	−10.974332	32.259457	−2.328826	3.970732
2:1:1	2	1	−11.346631	63.015304	−1.805872	1.664979
3:3:2	1.5	1.5	−14.430365	53.784051	−2.041479	3.091200
2:2:1	2	2	−18.430516	137.771800	−1.466654	1.278623

duced. Using Eq. (22) and following similar derivations as in Ref. [8], we find that the s-wave scattering length a_0 is related to the energy difference in a generic rectangular box via

$$\delta E=-\frac{2\pi a_0}{\eta_1\eta_2\mu L^3}\left[1+c_1(\eta_1,\eta_2)\left(\frac{a_0}{L}\right)+c_2(\eta_1,\eta_2)\left(\frac{a_0}{L}\right)^2+\cdots\right]. \tag{26}$$

Here, μ designates the reduced mass of the two particles whose mass values are m_1 and m_2, respectively. The energy shift $\delta E\equiv E-m_1-m_2$ where E is the energy eigenvalue of the two-particle state. The functions $c_1(\eta_1,\eta_2)$ and $c_2(\eta_1,\eta_2)$ are given by

$$c_1(\eta_1,\eta_2)=\frac{\hat{Z}_{00}(1,0;\eta_1,\eta_2)}{\pi\eta_1\eta_2},$$

$$c_2(\eta_1,\eta_2)=\frac{\hat{Z}_{00}^2(1,0;\eta_1,\eta_2)-\hat{Z}_{00}(2,0;\eta_1,\eta_2)}{(\pi\eta_1\eta_2)^2}, \tag{27}$$

where the subtracted zeta function is defined as

$$\hat{Z}_{00}(s,q^2;\eta_1,\eta_2)=\sum_{|\tilde{\mathbf{n}}|^2\neq q^2}\frac{1}{(\tilde{\mathbf{n}}^2-q^2)^s}. \tag{28}$$

In Table II, we have listed numerical values for the coefficients $c_1(\eta_1,\eta_2)$ and $c_2(\eta_1,\eta_2)$ under some typical topology. In the first column of the table, we tabulated the ratio for the three sides of the box: $\eta_1:\eta_2:1$. Note that for $\eta_1=\eta_2=1$, these two functions reduce to the old numerical values for the cubic box which had been used in earlier scattering length calculations.

It can be shown that contaminations from higher-angular-momentum scattering phases come in at even higher powers of $1/L$. For low relative momenta, the d-wave scattering phase behaves like $\tan\delta_2(q)\sim a_2k^5=a_2(2\pi/L)^5q^5$, with a_2 being the d-wave scattering length. If we treat the effects due to $\tan\delta_2$ perturbatively, we see from Eqs. (20) and (21) that, in Eq. (26), the functions c_1 and c_2 receive contributions that are proportional to (a_2/L^5), which is of higher order in $1/L$ for large L.

V. CONCLUSIONS

In this paper, we have studied two-particle scattering states in a generic rectangular box with periodic boundary conditions. The relations of the energy eigenvalues and the scattering phases in the continuum are found. These formulas can be viewed as a generalization of the well-known Lüscher's formulas. In particular, we show that the s-wave scattering length is related to the energy shift by a simple formula, which is a direct generalization of the corresponding formula in the case of cubic box. We argued that this asymmetric topology might be useful in practice since it provides more available low-lying momentum modes in a finite box, which will be advantageous in the study of scattering phase shifts at nonzero three-momenta in hadron-hadron scattering and possibly also in other applications.

ACKNOWLEDGMENTS

This work is supported by the National Natural Science Foundation (NFS) of China under grant No. 90103006, No. 10235040 and supported by the Trans-century fund from the Chinese Ministry of Education.

APPENDIX A

In this Appendix, some explicit formulas for the modified zeta function defined in Eq. (9) will be given. For convenience of analytic continuation, one first defines the heat kernel:

$$\mathcal{K}(t,\mathbf{x})=\frac{1}{(2\pi)^3}\sum_{\mathbf{n}}e^{i\tilde{\mathbf{n}}\cdot\mathbf{x}-t\tilde{\mathbf{n}}^2}$$

$$=\frac{\eta_1\eta_2}{(4\pi t)^{3/2}}\sum_{\mathbf{n}}e^{-(1/4t)(\mathbf{x}-2\pi\hat{\mathbf{n}})^2}. \tag{A1}$$

Here the first equality is the definition of the heat kernel $\mathcal{K}(t,\mathbf{x})$ while the second follows from Poisson's identity. The summations which appear in this formula run over all three-dimensional integers $\mathbf{n}\in\mathbb{Z}^3$ and the notation $\tilde{\mathbf{n}}$ and $\hat{\mathbf{n}}$ is defined as in Eq. (2). It is evident that the heat kernel $\mathcal{K}(t,\mathbf{x})$ is periodic in $\mathbf{x}$ with period $2\pi\hat{\mathbf{n}}$—i.e., $\mathcal{K}(t,\mathbf{x}+2\pi\hat{\mathbf{n}})=\mathcal{K}(t,\mathbf{x})$. Given a positive number $\Lambda>0$, we define the truncated heat kernel $\mathcal{K}^{\Lambda}(t,\mathbf{x})$ as

TABLE III. Reduced matrix elements $\mathcal{M}_{ll'}(\Gamma)$ for the symmetry group D_4 for irreducible representations A_1^+, A_2^-, and E^-. Here we have adopted the basis defined in Table I. For all representations, only the nonvanishing matrix elements up to $l=4$ are listed. The columns labeled as $|l\rangle$ and $|l'\rangle$ indicate the basis vectors in which the matrix element $\mathcal{M}_{ll'}(\Gamma)$ is calculated for each given representation.

Γ	$\lvert l\rangle$	$\lvert l'\rangle$	$\mathcal{M}_{ll'}(\Gamma)$
A_1^+	0	0	$\mathcal{W}_{00}$
	2	0	$-\mathcal{W}_{20}$
	2	2	$\mathcal{W}_{00}+\frac{2\sqrt{5}}{7}\mathcal{W}_{20}+\frac{6}{7}\mathcal{W}_{40}$
	4	0	$\mathcal{W}_{40}$
	4	2	$-\frac{6}{7}\mathcal{W}_{20}-\frac{20\sqrt{5}}{77}\mathcal{W}_{40}-\frac{15\sqrt{65}}{143}\mathcal{W}_{60}$
	4	4	$\mathcal{W}_{00}+\frac{20\sqrt{5}}{77}\mathcal{W}_{20}+\frac{486}{1001}\mathcal{W}_{40}+\frac{20\sqrt{13}}{143}\mathcal{W}_{60}+\frac{490\sqrt{17}}{2431}\mathcal{W}_{80}$
	$\mathring{4}$	0	$\frac{1}{\sqrt{2}}(\mathcal{W}_{44}+\mathcal{W}_{4-4})$
	$\mathring{4}$	2	$\frac{2\sqrt{10}}{11}(\mathcal{W}_{44}+\mathcal{W}_{4-4})-\frac{15}{11\sqrt{26}}(\mathcal{W}_{64}+\mathcal{W}_{6-4})$
	$\mathring{4}$	4	$\frac{27\sqrt{2}}{143}(\mathcal{W}_{44}+\mathcal{W}_{4-4})-\frac{6\sqrt{10}}{11\sqrt{13}}(\mathcal{W}_{64}+\mathcal{W}_{6-4})+\frac{21\sqrt{1870}}{4862}(\mathcal{W}_{84}+\mathcal{W}_{8-4})$
	$\mathring{4}$	$\mathring{4}$	$\mathcal{W}_{00}-\frac{4\sqrt{5}}{11}\mathcal{W}_{20}+\frac{54}{143}\mathcal{W}_{40}-\frac{4}{11\sqrt{13}}\mathcal{W}_{60}+\frac{7}{143\sqrt{17}}\mathcal{W}_{80}+\frac{21\sqrt{5}}{\sqrt{4862}}(\mathcal{W}_{88}+\mathcal{W}_{8-8})$
A_2^-	1	1	$\mathcal{W}_{00}+\frac{2}{\sqrt{5}}\mathcal{W}_{20}$
	3	1	$-\frac{3\sqrt{3}}{\sqrt{35}}\mathcal{W}_{20}-\frac{4}{\sqrt{21}}\mathcal{W}_{40}$
	3	3	$\mathcal{W}_{00}+\frac{4}{3\sqrt{5}}\mathcal{W}_{20}+\frac{6}{11}\mathcal{W}_{40}+\frac{100}{33\sqrt{13}}\mathcal{W}_{60}$
E^-	$\tilde{\underset{\sim}{1}}$	$\tilde{\underset{\sim}{1}}$	$\mathcal{W}_{00}-\frac{1}{\sqrt{5}}\mathcal{W}_{20}\mp\frac{\sqrt{3}}{\sqrt{10}}(\mathcal{W}_{22}+\mathcal{W}_{2-2})$
	$\tilde{\underset{\sim}{3}}$	$\tilde{\underset{\sim}{3}}$	$\mathcal{W}_{00}+\frac{1}{\sqrt{5}}\mathcal{W}_{20}+\frac{1}{11}\mathcal{W}_{40}-\frac{25}{11\sqrt{13}}\mathcal{W}_{60}$
			$\mp\frac{\sqrt{2}}{\sqrt{15}}(\mathcal{W}_{22}+\mathcal{W}_{2-2})\mp\frac{\sqrt{10}}{11}(\mathcal{W}_{42}+\mathcal{W}_{4-2})\mp\frac{5\sqrt{35}}{11\sqrt{39}}(\mathcal{W}_{62}+\mathcal{W}_{6-2})$
	$\tilde{\underset{\sim}{3}}$	$\tilde{\underset{\sim}{1}}$	$-\frac{3\sqrt{2}}{\sqrt{35}}\mathcal{W}_{20}+\frac{\sqrt{2}}{\sqrt{7}}\mathcal{W}_{40}\mp\frac{\sqrt{3}}{2\sqrt{35}}(\mathcal{W}_{22}+\mathcal{W}_{2-2})\pm\frac{\sqrt{5}}{2\sqrt{7}}(\mathcal{W}_{42}+\mathcal{W}_{4-2})$
	$\dot{\underset{\cdot}{3}}$	$\dot{\underset{\cdot}{3}}$	$\mathcal{W}_{00}-\frac{\sqrt{5}}{3}\mathcal{W}_{20}+\frac{3}{11}\mathcal{W}_{40}-\frac{5}{33\sqrt{13}}\mathcal{W}_{60}\mp\frac{35}{\sqrt{3003}}(\mathcal{W}_{66}+\mathcal{W}_{6-6})$
	$\dot{\underset{\cdot}{3}}$	$\tilde{\underset{\sim}{1}}$	$-\frac{3}{2\sqrt{7}}(\mathcal{W}_{22}+\mathcal{W}_{2-2})+\frac{1}{2\sqrt{21}}(\mathcal{W}_{42}+\mathcal{W}_{4-2})\pm\frac{1}{\sqrt{3}}(\mathcal{W}_{44}+\mathcal{W}_{4-4})$
	$\dot{\underset{\cdot}{3}}$	$\tilde{\underset{\sim}{3}}$	$-\frac{\sqrt{2}}{6}(\mathcal{W}_{22}+\mathcal{W}_{2-2})+\frac{3\sqrt{6}}{22}(\mathcal{W}_{42}+\mathcal{W}_{4-2})-\frac{5\sqrt{7}}{33\sqrt{13}}(\mathcal{W}_{62}+\mathcal{W}_{6-2})$
			$\pm\frac{\sqrt{42}}{22}(\mathcal{W}_{44}+\mathcal{W}_{4-4})\mp\frac{5\sqrt{35}}{11\sqrt{78}}(\mathcal{W}_{64}+\mathcal{W}_{6-4})$

TABLE IV. Reduced matrix elements $\mathcal{M}_{ll'}(\Gamma)$ for the symmetry group D_4 for irreducible representations E^+, $B_1^{\pm}$, $B_2^{\pm}$, and A_2^+.

Γ	$\lvert l\rangle$	$\lvert l'\rangle$	$\mathcal{M}_{ll'}(\Gamma)$
E^+	$\underset{\sim}{\tilde{2}}$	$\underset{\sim}{\tilde{2}}$	$\mathcal{W}_{00}+\frac{\sqrt{5}}{7}\mathcal{W}_{20}-\frac{4}{7}\mathcal{W}_{40}\mp\frac{\sqrt{30}}{14}(\mathcal{W}_{22}+\mathcal{W}_{2-2})\mp\frac{\sqrt{10}}{7}(\mathcal{W}_{42}+\mathcal{W}_{4-2})$
	$\underset{\sim}{\tilde{4}}$	$\underset{\sim}{\tilde{2}}$	$-\frac{\sqrt{30}}{7}\mathcal{W}_{20}-\frac{5\sqrt{2}}{77}\mathcal{W}_{40}+\frac{10\sqrt{6}}{11\sqrt{13}}\mathcal{W}_{60}$
			$\mp\frac{\sqrt{5}}{14}(\mathcal{W}_{22}+\mathcal{W}_{2-2})\pm\frac{9\sqrt{15}}{154}(\mathcal{W}_{42}+\mathcal{W}_{4-2})\pm\frac{2\sqrt{70}}{11\sqrt{13}}(\mathcal{W}_{62}+\mathcal{W}_{6-2})$
	$\underset{\sim}{\tilde{4}}$	$\underset{\sim}{\tilde{4}}$	$\mathcal{W}_{00}+\frac{17\sqrt{5}}{77}\mathcal{W}_{20}+\frac{243}{1001}\mathcal{W}_{40}-\frac{1}{11\sqrt{13}}\mathcal{W}_{60}-\frac{392}{143\sqrt{17}}\mathcal{W}_{80}$
			$\mp\frac{5\sqrt{30}}{77}(\mathcal{W}_{22}+\mathcal{W}_{2-2})\mp\frac{81\sqrt{10}}{1001}(\mathcal{W}_{42}+\mathcal{W}_{4-2})$
			$\mp\frac{\sqrt{105}}{11\sqrt{13}}(\mathcal{W}_{62}+\mathcal{W}_{6-2})\mp\frac{21\sqrt{140}}{143\sqrt{17}}(\mathcal{W}_{82}+\mathcal{W}_{8-2})$
	$\underset{\cdot}{\dot{4}}$	$\underset{\sim}{\tilde{2}}$	$-\frac{\sqrt{5}}{2\sqrt{7}}(\mathcal{W}_{22}+\mathcal{W}_{2-2})-\frac{5\sqrt{15}}{22\sqrt{7}}(\mathcal{W}_{42}+\mathcal{W}_{4-2})+\frac{2\sqrt{10}}{11\sqrt{13}}(\mathcal{W}_{62}+\mathcal{W}_{6-2})$
			$\pm\frac{\sqrt{15}}{11}(\mathcal{W}_{44}+\mathcal{W}_{4-4})\pm\frac{10\sqrt{3}}{11\sqrt{13}}(\mathcal{W}_{64}+\mathcal{W}_{6-4})$
	$\underset{\cdot}{\dot{4}}$	$\underset{\cdot}{\dot{4}}$	$\mathcal{W}_{00}-\frac{\sqrt{5}}{11}\mathcal{W}_{20}-\frac{81}{143}\mathcal{W}_{40}+\frac{17}{11\sqrt{13}}\mathcal{W}_{60}-\frac{56}{143\sqrt{17}}\mathcal{W}_{80}$
			$\mp\frac{\sqrt{21}}{\sqrt{143}}(\mathcal{W}_{66}+\mathcal{W}_{6-6})\mp\frac{14\sqrt{3}}{\sqrt{2431}}(\mathcal{W}_{86}+\mathcal{W}_{8-6})$
	$\underset{\cdot}{\dot{4}}$	$\underset{\sim}{\tilde{4}}$	$-\frac{3\sqrt{15}}{11\sqrt{14}}(\mathcal{W}_{22}+\mathcal{W}_{2-2})+\frac{27}{143\sqrt{14}}(\mathcal{W}_{42}+\mathcal{W}_{4-2})$
			$+\frac{3\sqrt{15}}{11\sqrt{13}}(\mathcal{W}_{62}+\mathcal{W}_{6-2})-\frac{42\sqrt{5}}{143\sqrt{17}}(\mathcal{W}_{82}+\mathcal{W}_{8-2})$
			$\pm\frac{27\sqrt{10}}{286}(\mathcal{W}_{44}+\mathcal{W}_{4-4})\pm\frac{3}{11\sqrt{26}}(\mathcal{W}_{64}+\mathcal{W}_{6-4})\mp\frac{42\sqrt{2}}{13\sqrt{187}}(\mathcal{W}_{84}+\mathcal{W}_{8-4})$
$B_{1/2}^+$	$\underline{\overline{2}}$	$\underline{\overline{2}}$	$\mathcal{W}_{00}-\frac{2\sqrt{5}}{7}\mathcal{W}_{20}+\frac{1}{7}\mathcal{W}_{40}\pm\frac{\sqrt{5}}{\sqrt{14}}(\mathcal{W}_{44}+\mathcal{W}_{4-4})$
	$\underline{\overline{4}}$	$\underline{\overline{4}}$	$\mathcal{W}_{00}+\frac{8\sqrt{5}}{77}\mathcal{W}_{20}-\frac{27}{91}\mathcal{W}_{40}-\frac{2}{\sqrt{13}}\mathcal{W}_{60}+\frac{196}{143\sqrt{17}}\mathcal{W}_{80}$
			$\pm\frac{81\sqrt{5}}{143\sqrt{14}}(\mathcal{W}_{44}+\mathcal{W}_{4-4})\pm\frac{3\sqrt{14}}{11\sqrt{13}}(\mathcal{W}_{64}+\mathcal{W}_{6-4})\pm\frac{21\sqrt{14}}{13\sqrt{187}}(\mathcal{W}_{84}+\mathcal{W}_{8-4})$
	$\underline{\overline{4}}$	$\underline{\overline{2}}$	$-\frac{\sqrt{15}}{7}\mathcal{W}_{20}+\frac{30\sqrt{3}}{77}\mathcal{W}_{40}-\frac{5\sqrt{3}}{11\sqrt{13}}\mathcal{W}_{60}$
			$\pm\frac{\sqrt{30}}{11\sqrt{7}}(\mathcal{W}_{44}+\mathcal{W}_{4-4})\mp\frac{5\sqrt{42}}{22\sqrt{13}}(\mathcal{W}_{64}+\mathcal{W}_{6-4})$
$B_{2/1}^-$	$\underline{\overline{3}}$	$\underline{\overline{3}}$	$\mathcal{W}_{00}-\frac{7}{11}\mathcal{W}_{40}+\frac{10}{11\sqrt{13}}\mathcal{W}_{60}\pm\frac{\sqrt{70}}{22}(\mathcal{W}_{44}+\mathcal{W}_{4-4})\pm\frac{5\sqrt{14}}{11\sqrt{13}}(\mathcal{W}_{64}+\mathcal{W}_{6-4})$
A_2^+	$\underset{\circ}{4}$	$\underset{\circ}{4}$	$\mathcal{W}_{00}-\frac{4\sqrt{5}}{11}\mathcal{W}_{20}+\frac{54}{143}\mathcal{W}_{40}-\frac{4}{11\sqrt{13}}\mathcal{W}_{60}+\frac{7}{143\sqrt{17}}\mathcal{W}_{80}-\frac{21\sqrt{5}}{\sqrt{4862}}(\mathcal{W}_{88}+\mathcal{W}_{8-8})$

$$\mathcal{K}^{\Lambda}(t,\mathbf{x})=\mathcal{K}(t,\mathbf{x})-\frac{1}{(2\pi)^3}\sum_{|\tilde{\mathbf{n}}|\leqslant\Lambda} e^{i\tilde{\mathbf{n}}\cdot\mathbf{x}-t\tilde{\mathbf{n}}^2}. \tag{A2}$$

We may apply the operator $\mathcal{Y}_{lm}(-i\nabla_{\mathbf{x}})$ to the heat kernels defined above. These are denoted as

$$\mathcal{K}_{lm}(t,\mathbf{x})=\mathcal{Y}_{lm}(-i\nabla_{\mathbf{x}})\mathcal{K}(t,\mathbf{x}),$$
$$\mathcal{K}^{\Lambda}_{lm}(t,\mathbf{x})=\mathcal{Y}_{lm}(-i\nabla_{\mathbf{x}})\mathcal{K}^{\Lambda}(t,\mathbf{x}). \tag{A3}$$

Using heat kernels defined above, one could rewrite the modified zeta function as

$$\mathcal{Z}_{lm}(s,q^2;\eta_1,\eta_2)=\sum_{|\tilde{\mathbf{n}}|\leqslant\Lambda}\frac{\mathcal{Y}_{lm}(\tilde{\mathbf{n}})}{(\tilde{\mathbf{n}}^2-q^2)^s}+\frac{(2\pi)^3}{\Gamma(s)}\int_0^\infty dt\,t^{s-1}e^{tq^2}\mathcal{K}^{\Lambda}_{lm}(t,\mathbf{0}). \tag{A4}$$

This expression is convergent as long as $\mathrm{Re}(s)>(l+3)/2$. Close to $t=0$, the function $e^{tq^2}\mathcal{K}^{\Lambda}_{lm}(t,\mathbf{0})$ behaves like

$$e^{tq^2}\mathcal{K}^{\Lambda}_{lm}(t,\mathbf{0})\sim\frac{\delta_{l0}\delta_{m0}\eta_1\eta_2}{(4\pi)^2t^{3/2}}+\mathcal{O}(t^{-1/2}). \tag{A5}$$

We may therefore analytically continue the zeta function by

$$\begin{aligned}\mathcal{Z}_{lm}(s,q^2;\eta_1,\eta_2)&=\sum_{|\tilde{\mathbf{n}}|\leqslant\Lambda}\frac{\mathcal{Y}_{lm}(\tilde{\mathbf{n}})}{(\tilde{\mathbf{n}}^2-q^2)^s}+\frac{(2\pi)^3}{\Gamma(s)}\Bigg\{\frac{\delta_{l0}\delta_{m0}\eta_1\eta_2}{(4\pi)^2(s-3/2)}\\&\quad+\int_0^1 dt\,t^{s-1}\left[e^{tq^2}\mathcal{K}^{\Lambda}_{lm}(t,\mathbf{0})-\frac{\delta_{l0}\delta_{m0}\eta_1\eta_2}{(4\pi)^2t^{3/2}}\right]\\&\quad+\int_1^\infty dt\,t^{s-1}e^{tq^2}\mathcal{K}^{\Lambda}_{lm}(t,\mathbf{0})\Bigg\},\end{aligned} \tag{A6}$$

which is a valid expression as long as $\mathrm{Re}(s)>1/2$. This completes the process of analytic continuation for the modified zeta functions. Using the explicit expression for $\mathcal{K}^{\Lambda}_{lm}(t,\mathbf{0})$, the integral from 0 to 1 in the above formula can be further simplified. After some manipulations, we find that the results, when combined with the finite summation, is convergent for all Λ. Therefore, we can now send Λ to infinity and drop the third integral. Since we are only concerned with modified zeta functions at $s=1$ or $s=2$, we will only give the expressions for these two cases. The final expression may be written as

$$\begin{aligned}\mathcal{Z}_{lm}(s,q^2;\eta_1,\eta_2)&=e^{q^2}\sum_{\mathbf{n}}\left[\frac{\mathcal{Y}_{lm}(\tilde{\mathbf{n}})}{(\tilde{\mathbf{n}}^2-q^2)^s}+\frac{(s-1)\mathcal{Y}_{lm}(\tilde{\mathbf{n}})}{(\tilde{\mathbf{n}}^2-q^2)^{s-1}}\right]e^{-\tilde{\mathbf{n}}^2}\\&\quad+\frac{\pi\eta_1\eta_2}{(2s-3)}\delta_{l0}\delta_{m0}+\frac{\pi\eta_1\eta_2}{2}\delta_{l0}\delta_{m0}\int_0^1 dt\,t^{s-5/2}\\&\quad\times(e^{tq^2}-1)+\pi\eta_1\eta_2\int_0^1 dt\,t^{s-5/2}\\&\quad\times\left[\sum_{\mathbf{n}\neq\mathbf{0}}\mathcal{Y}_{lm}\left(-i\frac{\pi}{t}\hat{\mathbf{n}}\right)e^{tq^2}e^{-(\pi^2/t)\hat{\mathbf{n}}^2}\right].\end{aligned} \tag{A7}$$

Note that this expression is valid only for $s=1$ or $s=2$.

APPENDIX B

In this Appendix, we list the reduced matrix elements that appeared in the formulas in the main text. We define

$$\mathcal{W}_{lm}(1,q^2;\eta_1,\eta_2)\equiv\frac{\mathcal{Z}_{lm}(1,q^2;\eta_1,\eta_2)}{\pi^{3/2}\eta_1\eta_2q^{l+1}}. \tag{B1}$$

Using this notation, we now proceed to list relevant reduced matrix elements $\mathcal{M}_{ll'}(\Gamma)$ for a given symmetry sector Γ. Here the labels l and l' designates the basis vectors defined in Table I. For the case of D_4 symmetry, up to angular momentum $l=4$, the nonvanishing matrix elements $\mathcal{M}_{ll'}(\Gamma)$ are listed in Tables III and IV.

For the case of D_2 symmetry, by comparing with Table I, one easily sees that the corresponding matrix elements are in fact the same as listed in Tables III and IV. The only difference is that the name of the irreducible representations are changed. For example, the matrix elements listed under E^- for D_4 symmetry are in fact corresponding matrix elements for the representations B_2^- and B_3^- for the D_2 symmetry, as suggested by Table I. Therefore, combining Tables I, III, and IV, we have all the reduced matrix elements for all irreducible representations up to $l\leqslant 4$ for both D_4 and D_2 symmetries.

[1] P. Truöl, hep-ex/0012012.
[2] M.J. Matison *et al.*, Phys. Rev. D **9**, 1872 (1974).
[3] N.O. Johannesson and J.L. Petersen, Nucl. Phys. **B68**, 397 (1973).
[4] A. Karabouraris and G. Shaw, J. Phys. G **6**, 583 (1980).
[5] A.D. Martin, Nucl. Phys. **B179**, 33 (1981).
[6] M. Lüscher, Commun. Math. Phys. **105**, 153 (1986).
[7] M. Lüscher and U. Wolff, Nucl. Phys. **B339**, 222 (1990).
[8] M. Lüscher, Nucl. Phys. **B354**, 531 (1991).
[9] M. Lüscher, Nucl. Phys. **B364**, 237 (1991).
[10] M. Goeckeler, H.A. Kastrup, J. Westphalen, and F. Zimmermann, Nucl. Phys. **B425**, 413 (1994).
[11] R. Gupta, A. Patel, and S. Sharpe, Phys. Rev. D **48**, 388 (1993).
[12] M. Fukugita, Y. Kuramashi, H. Mino, M. Okawa, and A. Ukawa, Phys. Rev. D **52**, 3003 (1995).

[13] S. Aoki *et al.*, Nucl. Phys. B (Proc. Suppl.) **83**, 241 (2000).
[14] S. Aoki *et al.*, Phys. Rev. D **66**, 077501 (2002).
[15] C. Liu, J. Zhang, Y. Chen, and J.P. Ma, Nucl. Phys. **B624**, 360 (2002).
[16] K.J. Juge, Nucl. Phys. B (Proc. Suppl.) **129**, 194 (2004).
[17] S. Aoki *et al.*, Phys. Rev. D **67**, 014502 (2003).
[18] N. Ishizuka and T. Yamazaki, Nucl. Phys. B (Proc. Suppl.) **129**, 233 (2004).
[19] T. Yamazaki *et al.*, Nucl. Phys. B (Proc. Suppl.) **129**, 191 (2004).
[20] S.R. Beane, P.F. Bedaque, A. Parreno, and M.J. Savage, Phys. Lett. B **585**, 106 (2004).
[21] N. Ishizuka, Nucl. Phys. B (Proc. Suppl.) **119**, 84 (2003).
[22] X. Li and C. Liu, Phys. Lett. B **587**, 100 (2004).
[23] M. Rotenberg, R. Bivins, N. Metropolis, and J.K. Wooten, Jr., *The 3-j and 6-j Symbols* (The Technology Press, Massachusetts Institute of Technology, Cambridge, MA, 1959).
[24] L.D. Landan and E.M. Lifshitz, *Quantum Mechanics*, 3rd ed. (Pergamon Press, Oxford, 1977).
[25] J.D. Jackson, *Classical Electrodynamics* (Wiley, New York, 1975).